Binding Properties of Ferrocene-glutathione Conjugates as Inhibitors and Sensors for Glutathione S-transferases

Manuel C. Martos-Maldonado,[a] Juan M. Casas-Solvas,[a,1] Ramiro Téllez-Sanz,[b] Concepción Mesa-Valle,[b] Indalecio Quesada-Soriano,[b] Federico García-Maroto,[c] Antonio Vargas-Berenguel,[a] and Luís García-Fuentes[b,*]

[a]Área de Química Orgánica, [b]Área de Química Física and [c]Área de Bioquímica y Biología Molecular, Faculty of Experimental Sciences, University of Almería, La Cañada de San Urbano, 04120 Almería, Spain.

[*]**Corresponding author:** Área de Química Física, Edificio de Química, University of Almería, La Cañada de San Urbano s/n, 04120 Almería, Spain. Fax: (+34) (950) 015008. Phone: (+34) (950) 015618. E-mail: lgarcia@ual.es.

Current address

[1]School of Chemistry, University of Bristol, Cantock's Close, Bristol, BS8 1TS, United Kingdom.

Abstract

The binding properties of two electroactive glutathione-ferrocene conjugates that consist in glutathione attached to one or both of the cyclopentadienyl rings of ferrocene (GSFc and GSFcSG), to *Schistosoma japonica* glutathione S-transferase (SjGST) were studied by spectroscopy fluorescence, isothermal titration calorimetry (ITC) and differential pulse voltammetry (DPV). Such ferrocene conjugates resulted to be competitive inhibitors of glutathione S-transferase with an increased binding affinity relative to the natural substrate glutathione (GSH). We found that the conjugate having two glutathione units (GSFcSG) exhibits an affinity for SjGST approximately two orders of magnitude higher than GSH. Furthermore, it shows negative cooperativity with the affinity for the second binding site two orders of magnitude lower than that for the first one. We propose that the reason for such negative cooperativity is steric since, i) the obtained thermodynamic parameters do not indicate profound conformational changes upon GSFcSG binding and ii) docking studies have shown that, when bound, part of the first bound ligand invades the second site due to its large size. In addition, voltammetric measurements show a strong decrease of the peak current upon binding of ferrocene-glutathione conjugates to SjGST and provide very similar *K* values than those obtained by ITC. Moreover, the sensing ability, expressed by the sensitivity parameter shows that GSFcSG is much more sensitive than GSFc, for the detection of SjGST.

Keywords: ferrocene-glutathione conjugates, binding, voltammetry, calorimetry, electrochemical sensors, docking, cooperativity, glutathione S-transferase.

1. Introduction

Reduced glutathione, most commonly named glutathione or GSH, is a relatively small molecule which is ubiquitous in living systems. GSH, a linear tripeptide composed by cysteine, glutamic acid and glycine, is an intracellular nucleophile and antioxidant that serves a protective and detoxifying function in the body. It is involved in phase II drug metabolism of reactive electrophiles and quenches free radicals and reactive oxygen species produced from endogenous and exogenous sources [1]. Glutathione levels in the cells are maintained in two ways: the *de novo* biosynthesis of glutathione from the constituent amino acids and the reduction of oxidized glutathione (GSSG) back to reduced glutathione (GSH) by glutathione reductase [2]. The glutathione S-transferases catalyze the conjugation of glutathione to different endogenous and exogenous electrophilic compounds [3-5]. The best known role of those enzymes is as cell housekeepers engaged in the detoxification of xenobiotics. Over-expression of GSTs was demonstrated in a number of different human cancer cells and has been considered as a diagnostic indicator of chemical carcinogenesis. It has been found that the resistance to many anticancer chemotherapeutics is directly correlated with the over-expression of GSTs in malign cells relative to their concentration in the corresponding normal tissue [6-8].The resistance is in part caused by an increased metabolic detoxication of the drugs in the cancer cells. Therefore, GST inhibition emerges as a good choice to decrease the resistance of cells to anticancer drugs. Many compounds have been described in the literature as GST inhibitors, including GSH analogs, GSH conjugates, small organic molecules and natural products [9-11]. Perhaps the most explored strategy for the development of GST inhibitors has been the conjugation of GSH, through its thiol group, to a variety of structural moieties. The rationale for this strategy is based on the observation that GSTs are subject to product inhibition [12].

Metallocenes exhibit a wide range of biological activity. Among them, ferrocene (Fc) has attracted a special attention in medicinal research since it is a neutral, chemically stable and nontoxic molecule with excellent redox properties. Conjugation of ferrocene with biomolecules such as DNA, amino acids and peptides is envisioned to provide novel systems depending on the properties of both types of molecules. Many ferrocenyl compounds display interesting cytotoxic, antitumor, antimalarial, antifungal and DNA-cleaving activity [13]. Their redox process is electrochemically reversible or quasireversible and their redox potential depends on the nature of substituents attached to the cyclopentadienyl rings. They have found applications in different fields such as biosensors, drug delivery systems, electrocatalyts and optoelectronics, among others.

Moreover, it is known that GSH does not show discernable voltammetric signals. Thus, voltammetric techniques, which are simple, sensitive and suitable for real time monitoring of chemical and biological reactions, cannot be used to examine the GST-GSH interactions. However, a frequent approach is to modify ligands by attaching to them a redox label, such as ferrocene, to enable their electrochemical detection. We have reported the synthesis of a series of water-soluble glycosyl ferrocene derivatives and the binding and redox sensing properties towards model receptors and a lectin [14, 15]. Recently, some authors have synthesized ferrocene-labeled glutathione, and they have studied its capability to inhibit equine liver GST by activity assays [16] and its interaction with bovine serum albumin [17]. However, to the best of our knowledge, neither thermodynamic nor voltammetric studies have been done with ferrocene-GSH derivatives and GST. To address the matter, we have synthesized two ferrocenyl derivatives conjugated with GSH and investigated their electrochemical behavior with the goal of using them as redox probes for the detection of GST.

For this purpose, we conducted a thermodynamic and electrochemical study on the GSFc and GSFcSG interactions with the GST enzyme. The results were compared to those obtained for their parent compounds (GSH and GSSG). The Fc-glutathione conjugates are competitive inhibitors of GST with an increased binding affinity relative to the natural substrate GSH.

2. Materials and methods

2.1. General methods. TLC was performed on Merck Silica Gel 60 F_{254} aluminium sheets and developed by UV light and ethanolic sulfuric acid (5 % v/v). Flash column chromatography was performed on Merck Silica Gel (230-400 mesh, ASTM). Melting points were measured on a Büchi B-450 melting point apparatus and are uncorrected. Optical rotations were recorded on a Jasco P-1030 polarimeter at room temperature. $[\alpha]_D$ values are given in 10^{-1} deg cm^2 g^{-1}. IR spectra were recorded on a Mattson Genesis II FTIR. ^1H, ^{13}C and 2D NMR spectra (gCOSY and gHMQC) were recorded on Bruker Avance DPX300 and Bruker Avance 500 Ultrashield spectrometers equipped with a QNP $^1H/^{13}C/^{19}F/^{31}P$ and an inverse TBI $^1H/^{31}P$/BB probe, respectively. Standard Bruker software was used for acquisition and processing routines. Chemical shifts are given in ppm and referenced to internal TMS (δ_H and δ_C 0.00). *J* values are given in Hz. ESI-TOF mass spectra were recorded on a Bruker Microtof spectrometer.

GSH (1), GSSG, (hydroxymethyl)ferrocene (2) and 1,1’ bis(hydroxymethyl)ferrocene (3) were purchased from Sigma-Aldrich. Ligand samples were prepared from powder stocks by adding an appropriate aliquot of material into the dialysis buffer. All other chemicals were of analytical grade of the highest available purity.

All solutions for calorimetric studies were made with distilled and deionized (Milli Q) water.

2.2. Synthesis of ferrocene-Glutatione conjugates

2.2.1. [(S-L-glutathionyl)methyl]ferrocene, (GSFc **4**). Compound **4** was prepared by using a modification of the method reported [16]. To a solution of glutathione (**1**) (50 mg, 0.163 mmol) in water (2 mL) was added a solution of (hydroxymethyl)ferrocene (**2**) (53 mg, 0.245 mmol) in ethanol (2 mL) and then trifluoroacetic acid (40 μL, 0.489 mmol). The mixture was stirred for 2 h 30 min at room temperature. Then, the pH was increased until 9-10 by adding saturated aqueous $NaHCO_3$. The solvent was removed by evaporation under vacuum and the crude was purified by column chromatography (CH_3CN/H_2O 5:1) to yield compound **4** (86 mg, 96 %) as a yellow solid: M. p. 211 ºC (dec.); $[\alpha]_D$ – 7.2 º (c 0.2, H_2O); IR (KBr, cm-1): 3278, 1644, 1594, 1540, 1409, 1311, 1244, 1142, 1112, 996, 924, 637, 623, 498, 484; ^{1}H-NMR (300 MHz, D_2O), δ (ppm): 4.43 (dd, 1H, ^3J = 8.7 Hz, ^3J = 4.9 Hz, α-Cys), 4.24 (bs, 2H, H_{Cp}), 4.18 (bs, 7H, H_{Cp}, $H_{Cp'}$), 3.72 (d, 1H, ^2J = 17.3 Hz, α-Gly), 3.67 (t, 1H, ^3J = 6.4 Hz, α-Glu), 3.64 (d, 1H, ^2J = 17.3 Hz, α'-Gly), 3.56 (bs, 2H, CH_2S), 2.96 (dd, 1H, ^2J = 14.1 Hz, ^3J = 4.9 Hz, β-Cys), 2.75 (dd, 1H, ^2J = 14.1 Hz, ^3J = 8.7 Hz, β'-Cys), 2.42 (t, 2H, ^3J = 7.2 Hz, γ-Glu), 2.09-2.02 (m, 2H, β-Glu); ^{13}C-NMR (75 MHz, D_2O), δ (ppm): 176.0, 174.7, 173.9, 171.8 (CO), 84.6 (C_{ipso}), 69.0, 68.8, 68.7, 68.5, 68.4 (C_{Cp}), 54.1 (α-Glu), 53.0 (α-Cys), 43.3 (α-Gly), 32.7 (β-Cys), 31.4 (CH_2S), 31.3 (γ-Glu), 26.2 (β-Glu); HMRS (ESI-TOF): Calc. for $C_{21}H_{27}FeN_3O_6S$ 505.0970. Found: 505.0957 $[M]^+$, 528.0840 $[M + Na]^+$.

2.2.2. 1,1'-Bis[(S-L-glutathionyl)methyl]ferrocene, (GSFcSG **5**). To a solution of glutathione (1) (137 mg, 0.447 mmol) in water (3 mL) was added a solution of 1,1'-

bis(hydroxymethyl)ferrocene (2) (50 mg, 0.203 mmol) in ethanol (1 mL) and then trifluoroacetic acid (64 μL, 0.831 mmol). The mixture was stirred for 5 h at room temperature. Then, the pH was increased until 9-10 by adding saturated aqueous $NaHCO_3$. The solvent was removed by evaporation under vacuum and the crude was purified by column chromatography (CH_3CN/H_2O 2:1) to yield compound **5** (161 mg, 87 %) as a yellow solid: M. p. 223 ºC (dec.); $[\alpha]_D$ – 13.7 º (c 0.2, H_2O); IR (KBr, cm-1): 3401, 1644, 1594, 1447, 1415, 1309, 1136, 1038, 1023, 879, 832, 621, 494; ^{1}H-NMR (300 MHz, D_2O), δ (ppm): 4.44-4.32 (dd, 1H, ^3J = 8.8 Hz, ^3J = 5.0 Hz, α-Cys), 4.20 (m, 4H, H_{Cp}), 4.17 (m, 4H, $H_{Cp'}$), 3.63 (d, 2H, ^2J = 17.3 Hz, α-Gly), 3.60 (d, 2H, ^2J = 17.3 Hz, α'-Gly), 3.40-3.22 (m, 2H, α-Glu), 3.56 (bs, 4H, CH_2S), 2.96 (dd, 2H, ^2J = 14.1 Hz, ^3J = 5.0 Hz, β-Cys), 2.74 (dd, 2H, ^2J = 14.1 Hz, ^3J = 8.8 Hz, β'-Cys), 2.43-2.19 (m, 4H, γ-Glu), 2.01-1.66 (m, 2H, β-Glu); ^{13}C-NMR (75 MHz, D_2O), δ (ppm): 176.1, 175.8, 171.9, 162.8 (CO), 85.0 (C_{ipso}), 69.6, 69.5, 69.4, 69.3 (C_{Cp}), 55.1 (α-Glu), 52.9 (α-Cys), 43.3 (α-Gly), 32.7 (β-Cys), 32.0 (CH_2S), 31.1 (γ-Glu), 29.6 (β-Glu); HMRS (ESI-TOF): Calc. for $C_{32}H_{44}FeN_6O_{12}S_2$ 824.1808. Found: 825.1859 $[M + H]^+$, 847.1677 $[M + Na]^+$.

2.3. Enzyme preparation and reactants. Recombinant *Schistosoma japonica* glutathione S-transferase (SjGST) was expressed and purified as described elsewhere [18]. After affinity purification, the enzyme was homogeneous as judged by SDS-PAGE. Protein concentration was measured at 278 nm using a molar extinction coefficient of 7.01×10^4 M^{-1} cm^{-1} for the dimer. Before use, the purified enzyme was concentrated and dialyzed at 4 °C against buffers. GST activity controls at 340 nm, according to Habig & Jakoby [19], were routinely performed before using the enzyme in the calorimetric experiments.

2.4. Fluorescence measurements. Intrinsic fluorescence of SjGST was measured with a PTI QuantaMaster (QM4-CW) spectrofluorometer equipped with a Peltier device and associated with a Biologic SFM/20 titration accessory. Excitation was at 278 ± 2 nm, and the emission was at 334 ± 2 nm. A number of samples containing 2-4 μM of GST in 2 mL of 20 mM sodium phosphate buffer (containing 5 mM NaCl, 0.1 mM EDTA) at pH 7 were added to a 3.0 mL quartz fluorescence cell and the fluorescence intensity measured. A suitable amount of the ligand (GSFc, GSSG, GSFcSG), dissolved in the same buffer was then added to each sample and the fluorescence intensity measured after mixing. The fluorescence intensities were measured in the range 300–350 nm. The fluorescence changes (ΔF) were calculated as F_0–F, where F is the fluorescence intensity of the sample solution and F_0 is the fluorescence of the protein in the absence of ligand, $F < F_0$. The measurements were corrected for dilution and inner filter effects. The procedure and data analysis used were similar to those described elsewhere [18].

2.5. Voltammetric experiments. Electrochemical measurements were carried out in sonicated, nitrogen-purged H_2O (MilliQ 18.2 MΩcm) solution with a microAutolab type III connected to a Intel Pentium Dual CPU 2.4 GHz personal computer running Eco Chimie B. V. GPES 4.9 software. The electrodes were carefully cleaned before each experiment. The glassy carbon disk working electrode (Ø 2 mm, effective area 0.038 ± 0.006 cm^2) was immersed in a 0.1 M HNO_3 solution for 5 min and polished with a basic Al_2O_3–water slurry The platinum sheet counter electrode (6 ± 4 mm, effective area 0.410 ± 0.003 cm^2) was immersed in a 50% v/v H_2SO_4 solution for 5 min.. Both electrodes were then sonicated in a 1:1:1 H_2O–MeOH–CH_3CN mixture for 5 min prior to use. The effective area of the electrodes was determined as previously reported [15]. A Ag/AgCl (3M KCl) electrode was

used as a reference. Differential pulse voltammetric (DPV) experiments were carried out in 10 mM phosphate buffer (pH 7.2) with 20 mM NaCl. Solutions of each conjugate (50 μM) and increasing amounts of SjGST varying from 0 to 90 μM were prepared in this buffer and shaken for 10 min at room temperature. Before each experiment, nitrogen was bubbled for 3 min. A DPV experiment was then measured between -200 mV and +600 mV with a scan rate of 5 mV s^{-1}, a step potential of 20 mV, a modulation amplitude of 50 mV, a modulation time of 0.05 s and an interval time of 2 s.

A two equal and independent sites model was used to fit the voltammetric data from GSFc while a two equal and interacting sites model was employed for GSFcSG. In the first case, the binding parameter, ν, defined as the ratio between the concentrations of bound ligand, $[L]_b$, and the total macromolecule, $[M]_t$, is expressed as:

$$\nu = \frac{2K[L]}{1+K[L]} \qquad (1)$$

where K and [L] are the equilibrium association constant and the free ligand concentration, respectively. However, a two equal and interacting sites model defines ν as

$$\nu = \frac{2K_1[L]+2K_1K_2[L]^2}{1+2K_1[L]+K_1K_2[L]^2} \qquad (2)$$

where K_1 and K_2 are the microscopic association constants for the first and second site, respectively.

Moreover, the concentration of free ligand is related to the total ligand, $[L]_t$, and the bound ligand, $[L]_b$, by the mass conservation law:

$$[L] = [L]_t - [L]_b \qquad (3)$$

Under the assumptions of a reversible, diffusion-controlled electron transfer and a diffusion coefficient for the bound ligand much lower than that for the free ligand, we can make the approximation of:

$$\frac{[L]}{[L]_t} = \frac{I}{I_0} \qquad (4)$$

where I and I_0 are the peak currents in the presence and in the absence of protein, respectively [14, 20]. Two algorithms, one with the equations (1), (3) and (4), and the other with (1), (2) and (4), were constructed using 'Scientist' software (Micromath Scientific Software, St. Louis, USA) to fit the experimental data of GSFc and GSFcSG, respectively.

2.6. Isothermal titration calorimetry. Calorimetric experiments were conducted using either a MCS [21] or an ultrasensitivity VP-ITC (Microcal Inc., Northampton, MA). The sample preparation and ITC experiments were carried out as previously described elsewhere [22]. Titrations were routinely performed in 20 mM sodium phosphate, 5 mM NaCl, 0.1 mM EDTA at pH 7. Phosphate buffer was chosen by virtue of its small ionization enthalpy change; hence, the binding enthalpies reported do not reflect the possible contribution due to buffer protonation. Blank titrations of ligand into buffer were also performed to correct for heat generated by dilution and mixing. Two models have been used to fit the experimental data: an equal and independent sites model (non-cooperative model) and a two equal and interacting sites model (cooperative model). The experimental data were fitted using 'Scientist' software (Micromath Scientific Software, St. Louis, USA) to the model algorithms implemented by us. The equations used in these models have been widely described in literature [23]. Finally, changes in the standard free energy ΔG^0 and entropy ΔS^0 were determined as $\Delta G^0 = -RT\ln K$ and $T\Delta S^0 = \Delta H - \Delta G^0$ (assuming that $\Delta H = \Delta H^0$).

2.7. Preparation of docking structures and analysis. GSSG, GSFc and GSFcSG structures were constructed by gluing together their moieties with the help of Avogadro 1.0 [24], taking special care in keeping the bond distances and angles at correct values. Ferrocene was taken from http://www.chemistry.nmsu.edu/studntres/Molecules/ferrocene.pdb and the G-site binding GS moiety from the pdb entry 1M99. We chose to proceed this way because we believe a structure coming from a crystallographic measurement is always better than a computer generated guess. We also used the ligand structures in other pdb entries like 3M8U and 1A3L as guides. In all of the cases the ligand G-site-binding GS moiety was taken from the pdb entry 1M99 after removing the sulfonate moiety from the crystallographic GS-conjugate. The SjGST protein structure was also taken from this pdb entry after removal of the ligand and water molecules.

AutoDockTools 1.5.4 [25] were used to prepare the protein and the ligands prior to the docking studies. Atomic Gasteiger partial charges and polar hydrogens were added. The protein structure was considered as a rigid body, as well as the ligands' G-site-binding GS moieties. The rest of the ligand structures were kept flexible with an automatic detection of the active rotatable bonds. The reason for keeping the G-site-binding GS moiety in the constructed ligands as unrotatable is due to the fact that its binding mode does not change regardless of the conjugate being bound to GST. This is easily seen when superimposing all of the corresponding published SjGST X-Ray structures (1M99, 1M9A, 1M9B and 1UA5). Thus, we chose to preserve this structure and leave it untouched by the docking process. In the particular case of the GSFcSG ligand, it is known the cyclopentadienyl rings can freely rotate around the ring centroid-Fe-ring centroid axis [26, 27]. However, it is not known which relative angle between the GS branches the GSFcSG ligand will have when bound to

the protein. As the docking process cannot freely rotate the cyclopentadienyl rings above the Fe atom, so we were forced to choose a fixed angle when constructing the ligand structure. Hence, we decided to create three different structures with three different dihedral angles between the GS branches (32.5º, 99.3º and 176.5º, respectively) using the relative orientation of the cyclopentadienyl rings in the ferrocene moiety taken from the ferrocene pdb.

To model the SjGST interaction with the GSSG, GSFc and GSFcSG conjugates, docking experiments were performed with AutoDock Vina 1.1.1 [28], which is based on the Iterated Local Search global optimizer algorithm [29, 30]. The runs were performed with an exhaustiveness of 256 and the search space centered in a subunit active site with widths of 16, 20 and 18 Å for the *x*, *y* and *z* axis, respectively. This box covers the whole G and H sites.

In order to select the best ligand binding conformations among the candidates proposed by Vina, we were guided by the binding mode of the ligand GS moiety in the G-site. When this binding mode exactly superimposes that of the crystallographic structures we would keep the pose as a hit. In the case of the GSFcSG ligand none of the 200+ analyzed poses for each relative angle between the GS branches gave an exact match, but however the 99.3º and 176.5º structures gave very similar conformations, with RMSD values less than 1. However, it is worth mentioning that, although not exactly matching the GS binding mode in the G-site, the selected hits from those structures matched each other regarding the GS moiety binding to the H-site. No single pose could be selected from the 32.5º structure. This suggests the real relative angle between the GS branches in this ligand when bound to SjGST probably lies between 90 and 180º.

3. Results and discussion

3.1. Synthesis. Alkylthiolation of the 1-ferrocenylmethyl position by direct reaction between the alkylthiol and the hydroxymethylferrocene derivative in acidic media is relatively easy due to the electrophilic reactivity of such position [15]. Thus, treatment of hydroxymethylferrocenes **2** and **3** and GSH (**1**) with TFA in a mixture of water/ethanol at room temperature led to the (*S*-glutathionylmethyl)ferrocene (GsFc **4**) [16] and bis(*S*-glutathionylmethyl)ferrocene (GSFcSG **5**) in 96 and 87% yields (Scheme 1).

3.2. Binding ability. It is widely known that GSTs have at least two ligand binding sites per monomer, G and H. The G-site is very specific for glutathione whereas the binding site for the xenobiotic substrate (H-site) is less specific in keeping with the ability of GSTs to react with a wide variety of toxic agents. Thus, in the case of these GSH-ferrocene conjugates the Fc moiety most likely will be filling the hydrophobic H-site. A further binding site was characterized based on the crystal structure of *Schistosoma japonica* GST complexed to the drug praziquantel [31]. The binding site, (named as "ligandin", "nonsubstrate" or "L-site") is located at the dimer interface and is thought to be the site of binding of large molecules including heme and bile salts [18, 32].

The binding of these inhibitors to GST quenches the intrinsic fluorescence of the enzyme as described for wt-GSH [33] and other inhibitors [22, 34]. We have performed an isothermal titration calorimetry study of the interaction between the ferrocene-glutathione conjugates (GSFc **4**, GSFcSG **5**) and dimeric SjGST. The results have been compared to those determined for the binding of GSH substrate [33] and oxidized glutathione (GSSG) to this enzyme. GSSG is both the substrate of glutathione reductase enzyme and a competitive inhibitor of glutathione S-transferase [35, 37]. Figure 1 shows representative titrations of SjGST with GSFc and GSSG at pH 7 and 25 ºC. The stoichiometry (*n*), enthalpy change

(ΔH) and binding constant, *K*, of the enzyme–ligand interactions were directly obtained from the shown experimental titration curves. In each case the top panel shows the raw calorimetric data, whilst the bottom panel plots the amount of heat generated per injection as a function of the molar ratio of glutathione conjugate to the enzyme. The solid line is the best fit of the experimental data to a non-cooperative model. Notably, no evidence for ligand binding cooperativity was observed. This model was clearly adequate to describe the binding between these ligands and SjGST, giving acceptable χ^2 values. As can be visualized in Figure 1, the binding of these ligands is always exothermic (negative peaks), with a stoichiometry approximately equal to 2 molecules of ligand per dimer (one ligand per subunit). Titrations of the enzyme with GSFc by fluorescence spectroscopy resulted in quenching curves that are consistent with the behavior obtained by calorimetry. The results deduced at 25 ºC are shown in Table 1. Figure 2 shows a typical ITC profile for the binding of GSFcSG to dimeric wt-SjGST in phosphate buffer at pH 7.0 and 25.1°C. Analogous experiments to those shown in Figures 1 and 2 were carried out in the temperature range of 15°–30°C. Control experiments that involve the same type of injections of conjugate solution into the same buffer were also carried out in order to measure the heat of dilution. A noncooperative model is inadequate to fit the experimental data for the GSFcSG binding, but a model of two equal and interacting sites fits them. The difference between both fits can easily be seen *ad oculus* in Figure 2. Therefore, the analysis of the GSFcSG and GSFc bindings to SjGST by ITC revealed two binding sites that displayed cooperative binding for GSFcSG but not for GSFc. The binding of GSFc was characterized by a microscopic binding constant (*K*) of 8.6×10^4 M^{-1} (K_d = 11.6 μM) and an enthalpy change of -7.9×10^3 kcal mol^{-1} for both binding sites at 25 ºC. Thus, the affinity of GSFc is one order of

magnitude higher than GSH [33]. This affinity is slightly lower than that calculated from inhibition assays with GST from equine liver (K_i ~ 4 μM) [16]. Moreover, some past findings indicated that the binding of GSH or GSSG to glutathione S-transferase A from rat liver occurred with very similar affinity (K_d = 7.06 ± 1.47 μM for GSH and K_d = 7.47 ± 0.31 μM for GSSG) [35]. These authors explained their results indicating the possibility that both ligands bind to the same site and that GSSG was bound only with one tripeptide moiety to the enzyme. Our results do not agree with these findings and suggest that GSSG binds to the H- and G-sites, similarly to other GS-conjugates [22, 38, 39], a binding mode supported by our docking studies (data not shown). The higher affinity of GSH-conjugates compared to its parent substrate (GSH) is also widely demonstrated in the literature [22, 39-41].

The GSFcSG conjugate binds cooperatively to the enzyme with two microscopic binding constants of 5.1×10^5 M^{-1} (K_1) and 9.9×10^3 M^{-1} (K_2) at 25 ºC. Thus, the binding equilibrium constant value for the first site, K_1, is approximately 2 orders of magnitude higher than that for the second site, K_2 (Table 1). Therefore, the GSFcSG affinity for the first site increases compared to that for GSFc. Consequently, GSFcSG is a better inhibitor of GST than the latter. Both binding processes are characterized by a favorable enthalpy change but an unfavorable entropy change.

The higher affinity of these conjugates (GSFc, GSSG and GSFcSG), compared to GSH, is a consequence of a more favorable enthalpy change, whilst the entropy changes are more unfavorable. An analogous result was also deduced for the binding of S-alkyglutathiones to SjGST [41]. On the other hand, the higher affinity of GSFcSG compared to GSSG comes from a more favourable enthalpy contribution and a less

negative entropy change (Table 1). It is also very important to underline that the GSFc affinity is 2-fold higher than that for GSSG. The reason for the higher affinity of GSFc compared to GSSG is entropic. The Gibbs binding energy decreases (becomes more favorable) as a consequence of the presence of the Fc moiety in the GS-conjugate, and so the affinity of GSFc to GST is higher than that for GSSG. These results suggest that although the interaction between the GSSG and the enzyme is enthalpically more favourable than that for GSFc, the entropic loss due to binding is also increased, indicating that the ferrocene moiety in the conjugate is enthalpically unfavorable but entropically favourable. The less unfavourable entropy change outweighs the enthalpic advantage, resulting in an affinity higher for the binding of GSFc. We propose that those differences come from higher hydrophobic character of the ferrocene group than that of the GS-moiety in these GS-conjugates. In those cases, analogously to other GS-conjugates [22, 38, 39, 42], Fc and other GS-bound moieties of the inhibitors fill the H-site of the enzyme, whereas the GSH moiety fills the G-site. Clearly, the resulting thermodynamic parameters values are a net balance of the interaction with both sites. Therefore, the difference in affinity between GSFc and GSSG comes from the more favorable entropy change in the case of GSFc (Table 1).

3.3. Temperature dependence. We analysed the interaction between SjGST and the three GS-conjugates mentioned above in phosphate buffer as a function of temperature between 15 and 30 °C at pH 7. The thermodynamic parameters derived from the temperature-dependent titration are displayed in Figure 3 and Table 2.

In all of the cases, whereas ΔG^0 remains practically invariant across the temperature range, the ΔH and ΔS^0 values are always negative and decrease as the temperature

increases. Hence, ΔG^0 of binding is exclusively contributed by a favorable ΔH. Van der Waals interactions and hydrogen bonding are usually considered to be the major potential sources of negative ΔH values [43]. As can be seen from the thermodynamic parameters displayed in Figure 3 and Table 2, we suggest that Van der Waals interactions and hydrogen bonds play a fundamental role in the interactions between these inhibitors and SjGST. Before binding, the inhibitor might be forming H-bonds with the water molecules in the solvent. After binding, the inhibitor might also be forming hydrogen bonds with the active site residues. Although the three-dimensional structures of these inhibitor-GST complexes have not been determined yet, the structures of GSH–enzyme and S-hexylglutathione-enzyme are known [31, 42]. In these structures several H-bonds have been described which may also exist in these enzyme–inhibitor complexes. These H-bonds are formed in a more apolar medium than water and may be the major contribution to the observed enthalpy change obtained. An increase in the apolarity of the moiety bound to GSH in the inhibitor produces a more hydrophobic environment, which could explain why the more apolar the ligand, the more negative the enthalpy change. Since the increase in affinity is caused by a more favorable enthalpic contribution, the H-bonds in a more hydrophobic environment may explain the higher affinity for the GSFcSG derivative.

Furthermore, the sign of the observed entropic change on binding provides some clues to the kind of physical processes involved. The main contributors to a negative entropy change are the hydrogen bond formation, a decrease in the number of isoenergetic conformations, and a decrease in soft internal vibrational modes [43]. For these inhibitors entropy remains negative at all of the temperatures studied, but for GSH the entropy change is positive at temperatures below 293.6 K. The entropy change values obtained for the three

inhibitors (Table 1) seem to indicate that there is no significant increase in the number of the hydration water molecules released regardless of the apolarity of the inhibitor.

Figure 3 shows a linear dependence of ΔH on temperature across the studied range, from the slope of which the heat capacity change is calculated. The binding of SjGST to these inhibitors involves negative changes in heat capacity (Table 1), which are frequent in binding studies and are a distinctive feature of site-specific binding [22, 41, 43]. The GSFc–SjGST interaction results in a ΔC_p value (−211 cal mol^{-1} K^{-1}) very similar to that for the oxidized form of glutathione (-209 cal mol^{-1} K^{-1}), but different to that obtained for GSFcSG–SjGST interaction (−145 cal mol^{-1} K^{-1}). This may suggest differences in the binding processes between these inhibitors. However, a high affinity binding and large negative ΔC_p are not necessarily correlated [41, 44]. Our results support this conclusion, showing that the higher binding affinity of GSFcGS is obtained with a lower heat capacity change. A large negative heat capacity change results from the formation of an 'intimate complementary interface of a ''specific'' complex' and is 'not a consequence of a high affinity reaction *per se'* [44].

The main difference in the binding of these GS-ferrocene conjugates to SjGST is the existence of negative cooperativity in the GSFcSG binding at all of the studied temperatures. When analyzing together the size of this inhibitor, the enzyme structure and the potential binding mode, a probable negative cooperativity may be reasonably predicted. Our docking studies, as explained below, reinforced this assumption, which was then confirmed calorimetrically. Negative and small heat capacity changes, such as those obtained in this study (included that deduced for GSFcSG), are usual in intrinsic binding processes but not in cooperative processes where the ligand binding induces profound

conformational changes affecting the other subunits. In those cases, cooperative processes accompanied by induced structural changes are frequently associated to higher ΔC_p values (positives or negative) [22, 34, 45, 46].

3.4. Docking studies. Since the GSFcSG ligand binds in a negative cooperativity fashion to SjGST and the thermodynamic results seem to indicate that there is no conformational change in the protein structure, we thought that the reason for this might be a steric hindrance for the binding of the second ligand molecule induced by the binding of the first. In order to address this question, we did a series of docking studies for the binding of GSSG, GSFc and GSFcSG.

Our docking results show a plausible origin for the negative cooperativity in the binding of GSFcSG to SjGST. Figure 4 depicts in a dark pink color one of the hit poses obtained for this ligand according to the criterion explained in the Materials and methods section, whilst a second ligand molecule occupying the other subunit of the binding site is depicted in a semi-transparent yellow color. The surface of the G-site residues of the displayed subunit appears as a green patch but the other SjGST subunit is omitted for clarity. The figure was made by removing the ligandless protein subunit in the docked ligand-SjGST complex and applying afterwards the symmetry operations indicated in the original pdb entry (1M99) to the remaining complex structure to construct the dimer. It is clear from the figure that the whole Gly and a part of the Cys in the H-site-bound tripeptide moiety of the GSFcSG ligand are overlapping the matching moiety of the second ligand molecule bound to the other protein subunit. The overlapping region lays on the ligandin or L-site, located at the dimer interface, where the praziquantel inhibitor binds (pdb entry 1GTB) [31]. We propose that the reason for the observed negative cooperativity is this

steric hindrance since, when bound, part of the first bound ligand invades the second ligand's binding site due to its large size.

It is interesting to note that, although the real relative angle between both GS branches in the GSFcSG ligand when bound to the SjGST protein is unknown, the ligand H-site-bound GS moiety binding mode is the same in all of the hit poses obtained for the 99.3º and 176.5º angles. According to these poses, this GS moiety is locked into position inside a subunit H-site through a 2.2 Å hydrogen bonding between the protonated Arg108 from the adjacent subunit and the terminal carboxylic acid of the GS-moiety glutamine.

It is also worth mentioning that, even if the docked pose of the G-site-bound GS moiety of this ligand does not exactly mimic the binding mode of GSH alone or its conjugates in other pdb entries (1M99, 1M9A, 1M9B and 1UA5), the docked binding mode is very similar (RMSD = 0.94 $Å^2$). Figure 4 shows how the docked ligand fits well in the green patch representing the G-site-residues surface, although the match is not perfect. The difference between our docked G-site binding modes for this ligand and the above mentioned pdb entries may arise from the fact that none of the chosen relative angles for the docking studies between both GS branches in the ligand is the real one when bound. Thus, such lack of perfect match in the G-site does not invalid the above reasoning on the origin of the negative cooperativity.

In the case of the GSSG and GSFc ligands, the same analysis indicates that such steric hindrance is not present, and the second ligand molecule can mimic the binding pose of the first without overlapping each other. This is in agreement with our thermodynamic results for which a two equal and independent binding sites model is able to fit the experimental data.

3.5. Voltammetric studies. The electrochemical properties of ferrocene-glutatione conjugates **4** and **5** have be studied by differential pulse voltammetry (DPV). DPV were performed using solutions of the conjugates (50 μM) prepared in water with 20 mM NaCl as a supporting electrolyte and using a glassy carbon working electrode, a Ag/AgCl (3 M KCl) reference electrode, and a Pt sheet counter electrode. The differential pulse voltammograms of **4** and **5** reveal only one oxidation peak for each ferrocene derivative, 0.220 V and 0.260 V, respectively, meaning that in aqueous solution the conjugates are present in only one distinguishable form. Such values are similar to those reported for thiomethylferrocene derivatives [15]. As expected, the oxidation potential value from the monosubstituted ferrocene GSFc **4** is lower than that from the ferrocene bearing two glutathione units. The different values are attributable to the different degrees of shielding of the ferrocene core by the peptide branches preventing solvent interactions [15]. As well, the peak current for GSFcSG **5** (0.801 μA) is almost half of the value for GSFc **4** (0.457 μA)**,** due to the larger size of the latter ferrocene derivative [15].

For the SjGST binding studies, we performed voltammetric measurements using solutions containing ferrocene–glutathione conjugates GSFc **4** and GSFcSG **5** (50 μM) and variable concentrations of SjGST (0–90 μM) after incubation for 10 min at room temperature. DPV voltammograms (Figures 5A and 5B) displays a progressive decrease of the peak current intensity as the SjGST concentration increases, while the oxidation potential does not change. This means that the binding of the Fc-glutathione conjugate to SjGST prevents the oxidation of the ferrocene moiety and the only available electroactive species remaining is the uncomplexed conjugate. As seen in Figures 5A and 5B, the

binding of GSFcSG **5** to SjGST causes a higher decrease of the peak current than that of GSFc **4**.

In order to obtain the *K* values of the binding interactions from the voltammetric data, the experimental peak current data were fitted *versus* the concentration of SjGST (see Figure 5C). In the case of GSFc **4**, the best fit of the experimental data to a non-cooperative model provides a *K* value of 2.06×10^4 M^{-1}, very similar to that obtained by ITC (see Table 1). By contrast, such a noncooperative model is inadequate to fit the experimental data obtained for the GSFcSG binding. As in the case of the ITC data (Table 1), a model of two equal and interacting sites is required to fit them, giving binding constants values of 8.3×10^5 M^{-1} (K_1) and 6.2×10^3 M^{-1} (K_2), also very close to those obtained from ITC.

3.6. Redox sensing abilities. Once we had demonstrated the protein-induced changes in the current peak intensity of the oxidation process of the Fc moiety in conjugates **4** and **5** upon binding to SjGST, we studied the sensing ability of the two conjugates. Whilst the thermodynamic and structural data described in previous sections are important from a molecular recognition viewpoint, from the sensing ability perspective it is desirable to use another type of assessment, such as that provided by a sensitivity parameter (P_s). This parameter would enable us to evaluate the extent of the peak current intensity variation induced by the conjugate-protein interaction. In our case, we defined the sensitivity parameter as $P_s = (I_0 - I)/I_0$, where I_0 and I denote the peak current intensity for the oxidation of the Fc moiety in the absence and the presence of SjGST, respectively. The sensitivity parameters P_s of both conjugates GSFc **4** and GSFcSG **5** are illustrated in Figure 6, which shows that GSFcSG **5** is much more sensitive than GSFc **4** for the detection of SjGST. But in the case of **5**, such increase is more rapid than that observed for the Ps value of **4**, particularly at lower concentrations of SjGST. After 50 μM of protein, the increase of

the Ps value for **5** slows down and the increase is slower than the Ps value for **4**. As displayed in Figure 6, P_s values for both conjugates increase as the SjGST concentration increases. The relative sensitivity of **4** and **5** to SjGST shows a clear correlation between the P_s and *K* values.

4. Conclusions

The binding of two electroactive glutathione-ferrocene conjugates (GSFc and GSFcSG) to SjGST were studied by spectroscopy fluorescence, isothermal titration calorimetry and voltammetry. The results have been compared to those obtained for their parent compounds (GSH and GSSG). The Fc-glutathione conjugates are competitive inhibitors of GST with an increased binding affinity relative to the natural substrate GSH. Fc-glutathione conjugate GSFcSG having two glutathione branches binds to the first protein monomer more strongly than the conjugate with only one peptide unit. However, GSFcSG shows negative cooperativity with the affinity for the second site two orders of magnitude lower than that for the first one. Calorimetric, voltammetric and fluorescence measurements provide very similar affinity values. The voltammetric studies have shown that both ferrocene–glutathione conjugates can be used as electrochemical sensors for the detection of SjGST, GSFcSG with two glutathione units being more sensitive for the detection of the protein. We suggest that the combination of its quasi 1:1 stoichiometry, enhanced voltammetric signal and high affinity makes GSFcSG a good redox probe for the electrochemical detection of GST levels.

Acknowledgements

The authors acknowledge the financial support from the Spanish Ministry of Science and Innovation and the EU European Regional Development Fund (Grant CTQ2010-17848), as well as the Andalusian Government (Consejería de Economía, Innovación y Ciencia-Junta de Andalucía, grant CVI-6028). The Spanish Ministry of Education is also acknowledged for a scholarship (M.C.M.-M.).

REFERENCES

[1] D.A. Dickinson, H.J. Forman, Cellular glutathione and thiols metabolism, Biochem. Pharmacol. 64 (2002) 1019–1026.

[2] D.M. Townsend, K.D. Tew, H. Tapiero, The importance of glutathione in human disease, Biomed. Pharmacother. 57 (2003) 145–155.

[3] R.N. Armstrong, Structure, catalytic mechanism, and evolution of the glutathione transferases, Chem. Res. Toxicol. 10 (1997) 2–18.

[4] J.D. Hayes, J.U. Flanagan, I.R. Jowsey, Glutathione transferases. Annu. Rev. Pharmacol. Toxicol. 45 (2005) 51–88.

[5] E. Laborde, Glutathione transferases as mediators of signaling pathways involved in cell proliferation and cell death. Cell Death Differ. 17 (2010) 1373–1380.

[6] U. Tidefelt, A. Elmhorm-Rosenborg, C. Paul, X.Y. Hao, B. Mannervik, L.C. Eriksson, Expression of glutathione transferase π as a predictor for treatment results at different stages of acute nonlymphoblastic leukemia, Cancer Res. 52 (1992) 3281–3285.

[7] D.J. Grignon, M. Abdel-Malak, W.C. Mertens, W.A. Sakr, R.R. Shepherd, Glutathione S-transferase expression in renal cell carcinoma: a new marker of differentiation, Mod. Pathol. 7 (1994) 186–189.

[8] R.E. Howells, K.K. Dhar, P.R. Hoban, P. W. Jones, A.A. Fryer, C.W. Redman, R.C. Strange, Association between glutathione-S-transferase GSTP1 genotypes, GSTP1 over-expression, and outcome in epithelial ovarian cancer, Int. J. Gynecol. Cancer 14 (2004) 242–250.

[9] S. Mahajan, W.M. Atkins, The chemistry and biology of inhibitors and pro-drugs targeted to glutathione S-transferases, Cell Mol. Life Sci. 62 (2005) 1221–1233.

[10] G.A. Morales, E. Laborde, Small-molecule inhibitors of glutathione S-transferase P1-1 as anticancer therapeutic agents, Annu. Rep. Med. Chem. 42 (2007) 321–335.

[11] P. Ruzza, A. Rosato, C.R. Rossi, M. Floreani, L. Quintieri, Glutathione transferases as targets for cancer therapy, Anti-Cancer Agents Med. Chem. 9 (2009) 763–777.

[12] D.J. Meyer, Significance of an unusually low K_m for glutathione in glutathione transferases of the α, μ and π classes, Xenobiotica 23 (1993) 823–834.

[13] M.F.R. Fouda, M.M. Abd-Elzaher, R.A. Abdelsamaia, A.A. Labib, On the medicinal chemistry of ferrocene, Appl. Organomet. Chem. 21 (2007) 613–625.

[14] J.M. Casas-Solvas, E. Ortiz-Salmerón, L. García-Fuentes, A. Vargas-Berenguel, Ferrocene-mannose conjugates as electrochemical molecular sensors for concanavalin A lectin, Org. Biomol. Chem. 6 (2008) 4230–4235.

[15] J.M. Casas-Solvas, E. Ortiz-Salmerón, J.J. Giménez-Martínez, L. García-Fuentes, L.F. Capitán-Vallvey, F. Santoyo-González, A. Vargas-Berenguel, Ferrocene-carbohydrate conjugates as electrochemical probes for molecular recognition studies, Chem.-Eur. J. 15 (2009) 710–725.

[16] B. Misterkiewicz, M. Salmain, G. Jaouen, Site-selective and covalent labelling of the cysteine-containing peptide glutathione with a ferrocenyl group, Tetrahedron Lett. 45 (2004) 7511–7513.

[17] Y. Peng, Y-N. Liu, F. Zhou, Voltammetric studies of the interactions between ferrocene-labeled glutathione and proteins in solution or immobilized onto surface, Electroanalysis 21 (2009) 1848–1854.

[18] Z. Yassin, E. Ortiz-Salmerón, F. García-Maroto, C. Barón, L. García-Fuentes, Implications of the ligandin binding site on the binding of non-substrate ligands to

Schistosoma japonicum-glutathione transferase, Biochim. Biophys. Acta 1698 (2004) 227–237.

[19] W.H. Habig, W.B. Jakoby, Assays for differentiation of glutathione S-transferases, Methods Enzymol. 77 (1981) 398–405.

[20] M.S. Ibraim, Voltammetric studies of the interaction of nogalamycin antitumour drug with DNA, Anal. Chim. Acta 443 (2001) 63–72.

[21] T. Wiseman, S. Williston, J.F. Brandts, L.N. Lin, Rapid measurement of binding constants and heats of binding using a new titration calorimeter, Anal. Biochem. 179 (1989) 131–137.

[22] I. Quesada-Soriano, L.J. Parker, A. Primavera, J.M. Casas-Solvas, A. Vargas-Berenguel, C. Barón, C.J. Morton, A.P. Mazzetti, M. Lo Bello, M.W. Parker, L. García-Fuentes, Influence of the H-site residue 108 on human glutathione transferase P1-1 ligand binding: structure-thermodynamic relationships and thermal stability, Protein Sci. 18 (2009) 2454–2470.

[23] J. Wyman, S.J. Gill, Binding and linkage: Functional Chemistry of Biological Macromolecules, University Science Books, Mill Valley, California 1990, pp 123–163.

[24] Avogadro: an open-source molecular builder and visualization tool. Version 1.01. http://avogadro.openmolecules.net/

[25] M.F. Sanner, Python: a programming language for software integration and development, J. Mol. Graphics Mod. 17 (1999) 57–61.

[26] E.W. Abel, N.J. Long, K.G. Orrell, A.G. Osborne, V. Šik, Dynamic NMR studies of ring rotation in substituted ferrocenes and ruthenocenes, J. Organomet. Chem. 403 (1991) 195–208.

[27] L.F.N. Ah Qune, K. Tamada, M. Hara, Self-assembling properties of 11-ferrocenyl-1-undecanethiol on highly oriented pyrolitic graphite characterized by scanning tunneling microscopy, e-J. Surf. Sci. Nanotech. 6 (2008) 119–123.

[28] O. Trott, A.J. Olson, AutoDock Vina: improving the speed and accuracy of docking with a new scoring function, efficient optimization and multithreading, J. Comput. Chem. 31 (2010) 455–461.

[29] J. Baxter, Local optima avoidance in depot location, J. Oper. Res. Soc. 32 (1981) 815–819.

[30] C. Blum, M.J. Blesa Aguilera, A. Roli, M. Sampels, Eds. Hybrid Metaheuristics: An Emerging Approach to Optimization, Springer-Verlag, Berlin, Heidelberg, 2008.

[31] M.A. McTigue, D.R. William, J.A. Tainer, Crystal structures of schistosomal drug and vacine target: glutathione S-transferase from *Schistosoma japonica* and its complex with the leading antischistosomal drug praziquantel, J. Mol. Biol. 246 (1995) 21–27.

[32] N. Sluis-Cremer, L. Wallace, J. Burke, J. Stevens, H. Dirr, Aflatoxin B1 and sulphobromophthalein binding to the dimeric human glutathione S-transferase A1-1: a fluorescence spectroscopic analysis, Eur. J. Biochem. 257 (1998) 434–442.

[33] E. Ortiz-Salmerón, Z. Yassin, M.J. Clemente-Jimenez, F.J. Las Heras-Vazquez, F. Rodriguez-Vico, C. Barón, L. García-Fuentes, Thermodynamic analysis of the binding of glutathione to glutathione S-transferase over a range of temperatures, Eur. J. Biochem. 268 (2001) 4307–4314.

[34] I. Quesada-Soriano, L.J. Parker, A. Primavera, J. Wielens, J.K. Holien, J.M. Casas-Solvas, A. Vargas-Berenguel, A.M. Aguilera, M. Nuccetelli, A.P. Mazzetti, M. Lo Bello, M.W. Parker, L. García-Fuentes, Diuretic drug binding to human glutathione transferase

P1-1: potential role of Cys-101 revealed in the double mutant C47S/Y108V, J. Mol. Recognit. 24 (2011) 220–234.

[35] I. Jakobson, M. Warholm, B. Mannervik, The binding of substrates and a product of the enzymatic reaction to glutathione S-transferase A, J. Biol. Chem. 254 (1979) 7085–7089.

[36] P. Askelöf, C. Guthenberg, I. Jakobson, B. Mannervik, Purification and characterization of two glutathione S-aryltransferase activities from rat liver, Biochem. J. 147 (1975) 513–522.

[37] T. Nishihara, H. Maeda, K. Okamoto, T. Oshida, T. Mizoguchi, T. Terada, Inactivation of human placenta glutathione S-transferase by SH/SS exchange reaction with biological disulfides, Biochem. Biophys. Res. Commun. 174 (1991) 580–585.

[38] A.J. Oakley, J. Rossjohn, M. Lo Bello, A.M. Caccuri, G. Federici, M.W. Parker, The three-dimensional structure of the human pi class glutathione transferase P1-1 in complex with the inhibitor ethacrynic acid and its glutathione conjugate, Biochemistry 36 (1997) 576–585.

[39] B.S. Nieslanik, C. Ibarra, W.M. Atkins, The C-terminus of glutathione S-transferase A1-1 is required for entropically-driven ligand binding, Biochemistry 40 (2001) 3536–3543.

[40] D.C. Kuhnert, Y. Sayed, S. Mosebi, M. Sayed, T. Sewell, H.W. Dirr, Tertiary interactions stabilise the C-terminal region of human glutathione transferase A1-1: a crystallographic and calorimetric study, J. Mol. Biol. 349 (2005) 825–838.

[41] E. Ortiz-Salmerón, Z. Yassin, M.J. Clemente-Jimenez, F.J., Las Heras-Vazquez, F. Rodriguez-Vico, C. Barón, L. García-Fuentes, A calorimetric study of the binding of S-

alkylglutathiones to glutathione S-transferase, Biochim. Biophys. Acta 1548 (2001) 106–113.

[42] R.M.F. Cardoso, D.S. Daniels, C.M. Bruns, J.A. Tainer, Characterization of the electrophile binding site and substrate binding mode of the 26-kDa glutathione S-transferase from *Schistosoma japonicum*, Proteins 51 (2003) 137–146.

[43] J.M. Sturtevant, Heat capacity and entropy changes in processes involving proteins, Proc. Natl. Acad. Sci. U. S. A. 74 (1977) 2236–2240.

[44] J.E. Ladbury, J.G. Wright, J.M. Sturtevant, P.B. Sigler, A thermodynamic study of the trp repressor-operator interaction, J. Mol. Biol. 238 (1994) 669–681.

[45] C. Barón, J.F. González, P.L. Mateo, M. Cortijo, Thermodynamic analysis of the activation of glycogen phosphorylase b over a range of temperatures, J. Biol. Chem. 264 (1989) 12872–12878.

[46] R. Téllez-Sanz, E. Cesareo, M. Nuccetelli, A.M. Aguilera, C. Barón, L.J. Parker, J.J. Adams, C.J. Morton, M., Lo Bello, M.W. Parker, L. García-Fuentes, Calorimetric and structural studies of the nitric oxide carrier S-nitrosoglutathione bound to human glutathione transferase P1-1, Protein Sci. 15 (2006) 1093–1105.

Table 1. Thermodynamic parameters of the binding of GSH and GS-ferrocene conjugates to SjGST at pH 7 and 25.2 ºC

Ligand	Fluorescence	Voltammetry	Calorimetry				
	$K \times 10^{-4}$ (M^{-1}]	$K \times 10^{-4}$ (M^{-1})	$K \times 10^{-4}$ (M^{-1})	$-\Delta G^0$ (kcal mol^{-1})	$-\Delta H$ (kcal mol^{-1})	$-T\Delta S^0$ (kcal mol^{-1})	$-\Delta C_p^0$ (cal K^{-1} mol^{-1})
[a]GSH	0.57 ± 0.20	-	0.38 ± 0.22	4.87 ± 0.16	5.71 ± 0.17	0.83 ± 0.16	238 ± 4
GSFc	9.5 ± 0.4	2.1 ± 0.9	8.6 ± 0.71	6.70 ± 0.10	7.92 ± 0.21	1.21 ± 0.32	211 ± 4
GSSG	3.9 ± 0.6	-	3.8 ± 0.8	6.24 ± 0.12	11.1 ± 0.10	4.90 ± 0.92	209 ± 6
GSFcSG	17 ± 1.5	83 ± 25	51 ± 31	7.72 ± 1.6	9.90 ± 0.17	2.13 ± 0.31	145 ± 34
	0.38 ± 0.18	0.62 ± 0.12	0.99 ± 0.32	5.42 ± 0.61	9.26 ± 0.28	3.83 ± 0.37	

[a]Data taken from [33]

Table 2. Thermodynamic parameters for GSSG and GSFcSG binding to SjGST at pH 7.0

Inhibitor	T (ºC)	$K \times 10^{-4}$ (M^{-1})	$-\Delta G^0$ (kcal mol^{-1})	$-\Delta H$ (kcal mol^{-1})	$-T\Delta S^0$ (kcal mol^{-1})
GSSG	16.1	7.4 ± 2.1	6.4 ± 0.5	9.2 ± 0.4	2.7 ± 0.3
	21.3	4.3 ± 1.6	6.2 ± 0.3	10.3 ± 0.3	4.1 ± 1.0
	25.3	3.9 ± 0.8	6.2 ± 0.1	11.1 ± 0.1	4.9 ± 0.9
	30.3	3.2 ± 1.2	6.2 ± 0.3	12.2 ± 0.3	5.9 ± 1.1
GSFcSG	15.2	45.2 ± 3.4	7.4 ± 1.1	5.8 ± 0.4	-1.7 ± 0.2
		1.4 ± 0.7	5.4 ± 0.3	12.3 ± 0.7	6.8 ± 1.2
	20.2	90.1 ± 5.7	7.9 ± 1.3	6.7 ± 0.5	-1.3 ± 0.2
		1.5 ± 1.2	5.6 ± 0.7	12.1 ± 0.5	6.5 ± 0.8
	25.1	50.6 ± 6.2	7.7 ± 1.6	9.9 ± 0.2	2.1 ± 0.3
		0.9 ± 1.1	5.4 ± 0.6	9.3 ± 0.3	3.8 ± 0.4
	30.0	56.0 ± 3.2	7.9 ± 1.0	12.3 ± 0.4	4.3 ± 0.6
		1.4 ± 1.1	5.7 ± 0.6	7.9 ± 0.4	2.2 ± 0.7

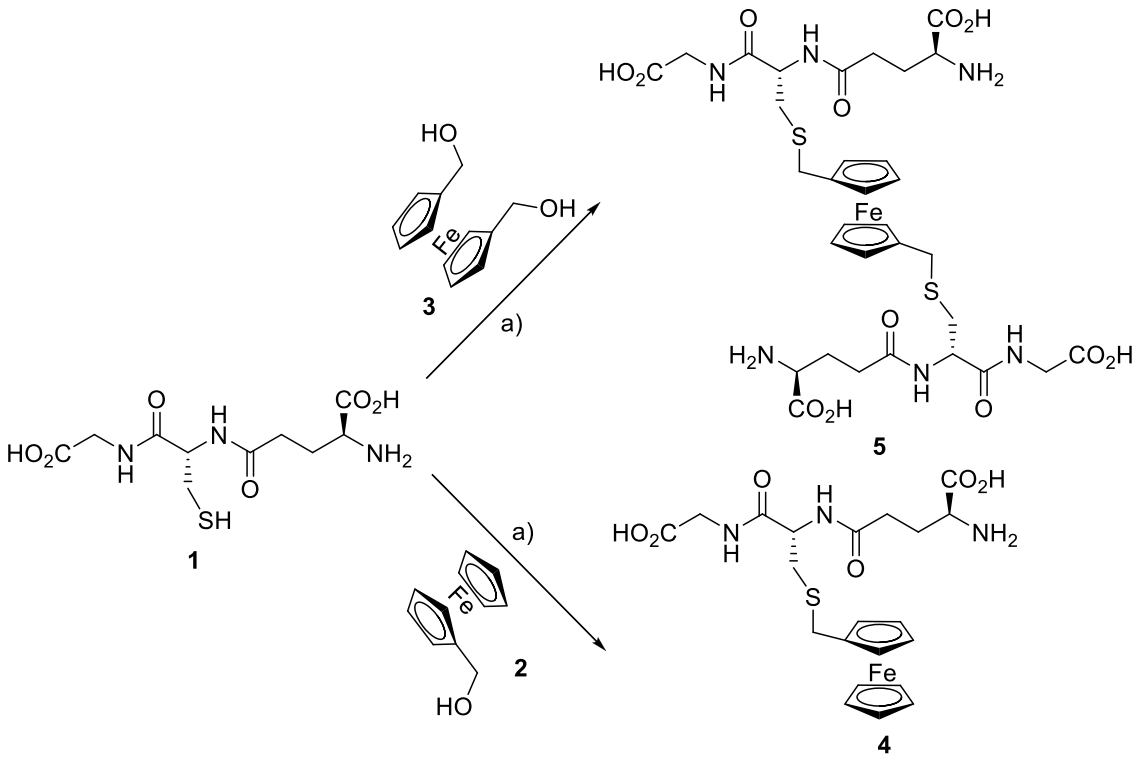

Scheme 1. Synthesis of glutathionylated ferrocenes **4** and **5**. Reagents and conditions: a) TFA, H_2O/EtOH, rt, 2.5-5 h., 96% (**4**) and 87 % (**5**).

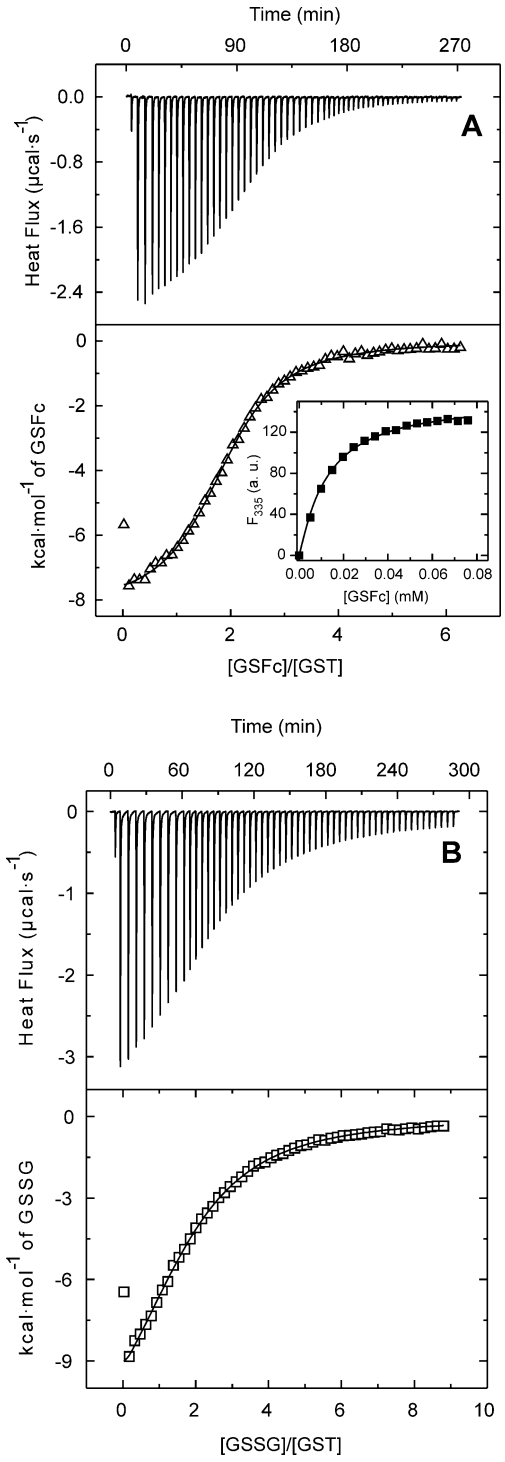

Figure 1. Representative isothermal titration calorimetry measurements of the binding of GSFc (A) and GSSG (B) to SjGST. **A**. Titration of 62.91 µM of dimeric SjGST with 58-5 µL injections of 1.75 mM GSFc. *Inset plot:* Titration by fluorescence. **B**. Titration of 52.11

μM of dimeric SjGST with 55-5 μL injections of 2.20 mM GSSG. A preinjection of 1 uL was performed at the beginning. Titrations were performed in 20 mM sodium phosphate, 5 mM NaCl and 0.1 mM EDTA at pH 7 and 25.1 ºC.

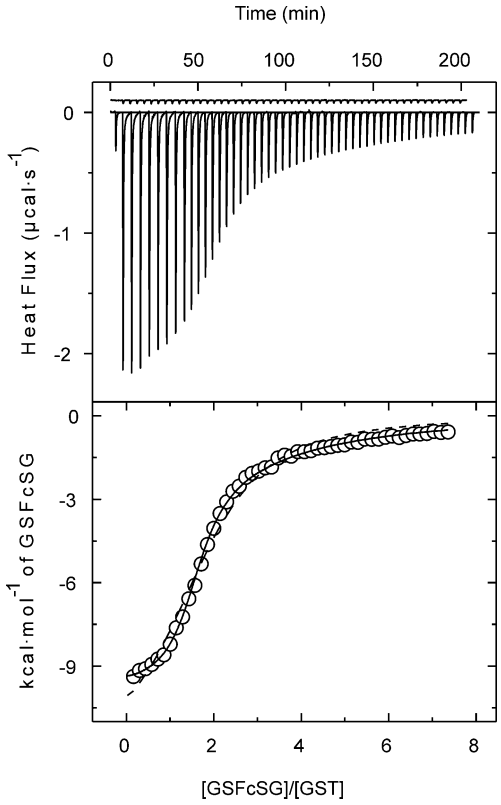

Figure 2. Representative isothermal titration calorimetry measurements of the cooperative binding of 1.4 mM GSFcSG to 54.9 μM dimeric SjGST. Bottom panel shows the fit to a cooperative model with $K_1 = 5.2 \times 10^5$ M^{-1}, $K_2 = 8.9 \times 10^3$ M^{-1}, $\Delta H_1 = -9.8$ kcal mol^{-1} and $\Delta H_2 = -9.2$ kcal mol^{-1}. The fitting to a non-cooperative model is also shown as dashed line. Titration was performed in 20 mM sodium phosphate, 5 mM NaCl and 0.1 mM EDTA at pH 7 and 25.1 ºC.

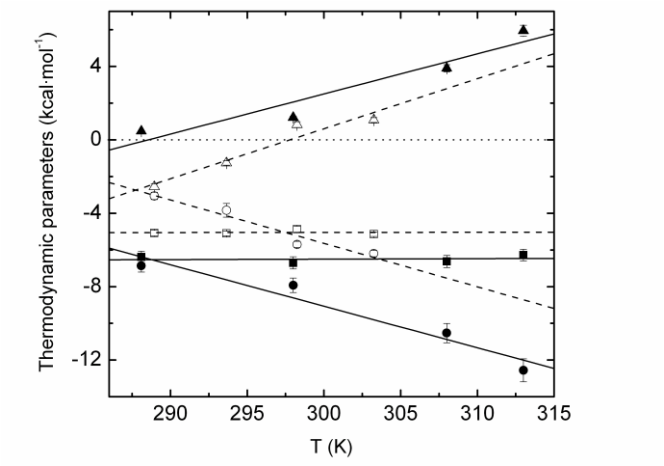

Figure 3. Temperature dependence of the thermodynamic parameters for binding of GSFc to dimeric SjGST**.** ΔG^0, ΔH and $-T\Delta S^0$ are shown as squares, circles and triangles, respectively. *Filled* and *open symbols* represent the parameters for GSFc and GSH binding, respectively. The heat capacity changes, associated with the binding, were determined by linear repression analysis as the slopes of the plots of ΔH. The parameters for GSH binding were taken from Ortiz-Salmerón et al. [33].

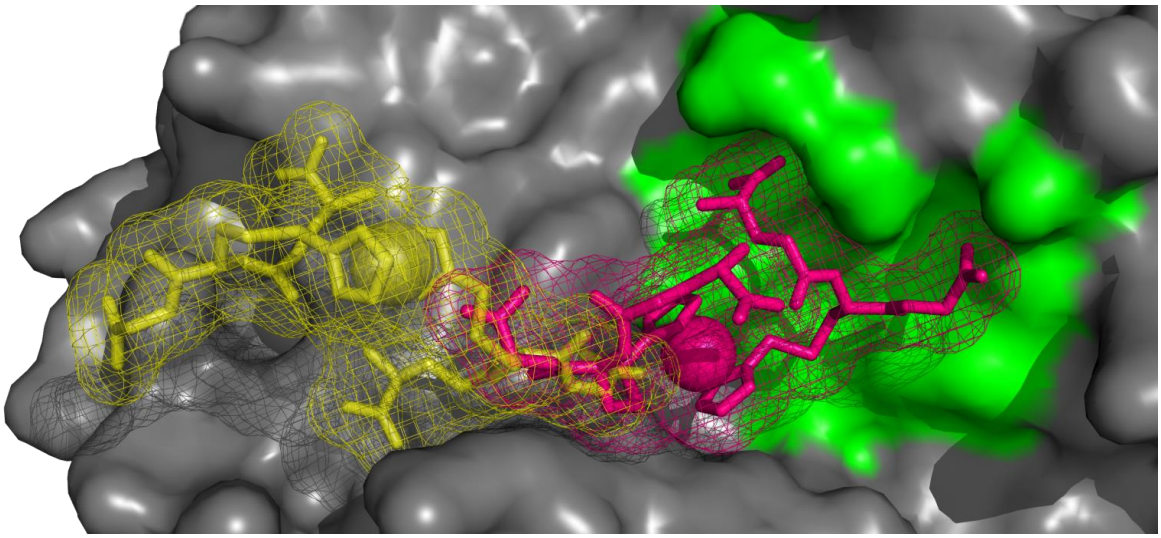

Figure 4. Predicted binding mode of GSFcGS into the SjGST dimer. The stick structure in a dark pink color represents the first molecule of this ligand bound to the enzyme. The binding subunit is depicted as a grey surface. The G-site in this subunit is shown as a green patch. The other subunit is above the plane shown and is omitted for the sake of clarity, but the second ligand molecule bound to it appears in a semi-transparent yellow color. It is clear there is some overlapping between both ligands at the region where the L-site lies.

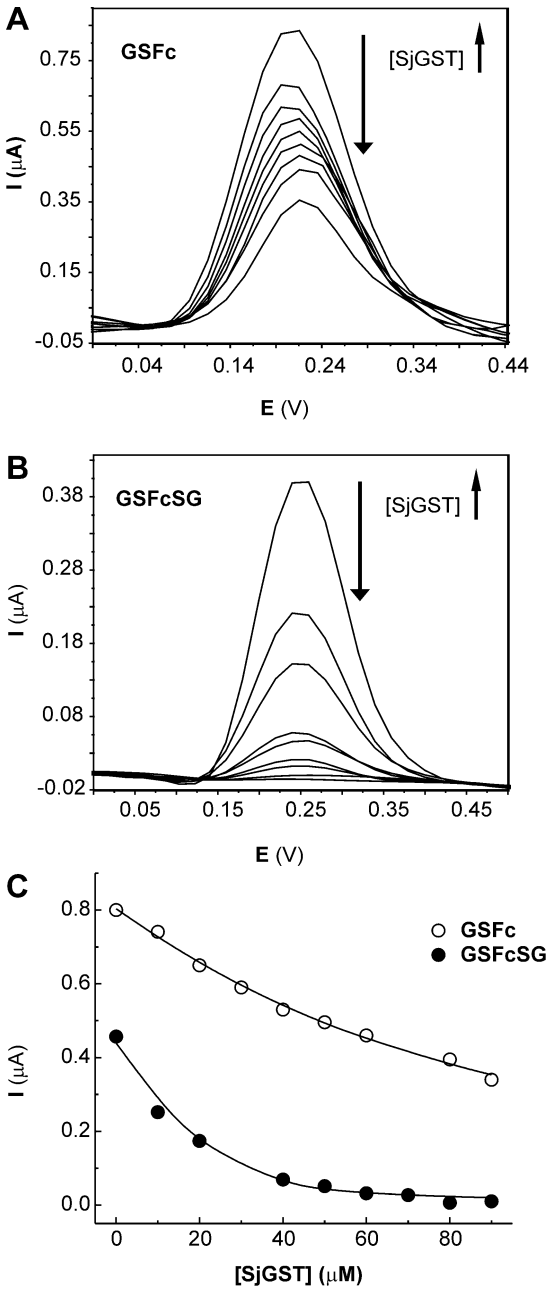

Figure 5. DPV curves for GSFc (A) and GSFcSG (B) (50 μM) in the presence of increasing amounts of SjGST ranging from 0 to 90 μM in 10 mM phosphate buffer (pH 7.2) with 20 mM NaCl. A decrease in the current (large arrow) was observed as SjGST concentration increased (small arrow). C) Graphical plot of peak current (DPV) of GSFc and GSFcSG (50 μM) versus concentration of SjGST (0−90 μM) in 10 mM phosphate

buffer (pH 7.2) with 20 mM NaCl. The smooth solid lines represent the best fit of the experimental data to the models of two equal and independent sites for GSFc and two equal and interacting sites for GSFcSG (see Materials and methods).

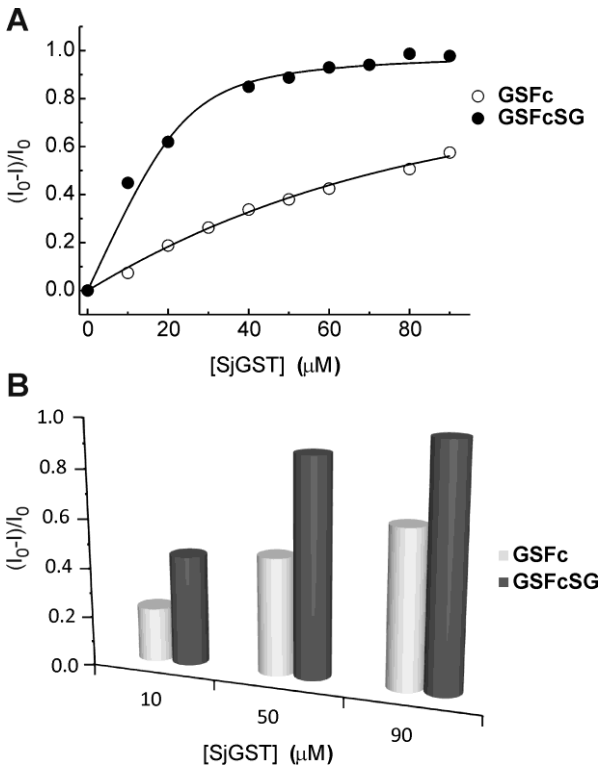

Figure 6. A) Evolution of sensitivity parameter values (Ps, $(I_0 – I)/I_0$) of GSFc and GSFcSG (50 μM) with the addition of increasing amounts of SjGST in 10 mM phosphate buffer (pH 7.2) with 20 mM NaCl. The smooth solid lines represent the best fit of the experimental data to the models implemented by us for two equal and independent sites in case of GSFc and for two equal and interacting sites in case of GSFcSG. B) Sensitivity parameter values of GSFc and GSFcSG (50 μM) in the presence of different concentrations of SjGST (10, 50 and 90 μM).

Graphical abstract: